Adsorption (2009) 15: 89–98
DOI 10.1007/s10450-009-9160-2

Heating effects on morphological and textural characteristics of individual and composite nanooxides

V.M. Gun'ko · R. Leboda · J. Skubiszewska-Zięba

Published online: 20 March 2009

Abstract Morphological, structural and adsorption characteristics of nanooxides (fumed individual silica, alumina and titania, and composite silica/alumina, silica/titania and alumina/silica/titania) were compared after different treatments (wetting/drying, ball-milling, suspending/drying, heating) at different temperatures (373–1173 K) using low-temperature nitrogen adsorption data. The structural characteristics such as specific surface area (S_{BET}), pore volume (V_p), pore (PSD) and particle (PaSD) size distributions (calculated using self-consisting regularization procedure with respect to both PSD and PaSD), fractality, adsorption energy distributions depend differently on heating temperature because desorption of water molecularly and dissociatively adsorbed at a surface and in bulk of primary nanoparticles occurs over a wide temperature range at different rates. These processes affect both structural and energetic characteristics of nanooxides.

Keywords Nanooxides · Morphology · Structural characteristics · Adsorption characteristics · Temperature effects

1 Introduction

Morphological, textural and adsorptive characteristics of nanooxides possessing a structural hierarchy with proto- (1–2 nm), primary (5–100 nm), secondary (<0.1–1 μm), ternary (1–10 μm) and quaternary (>10 μm) particles depend on flame synthesis conditions (flame temperature, its gradient, flame length, flow velocity and turbulence, ratio of reactant concentrations), phase distributions for composite oxides, amount of adsorbed water, and sample history (Iler 1979; Legrand 1998; Basic Characteristics of Aerosil 1997; Gun'ko et al. 2003, 2004, 2005, 2007a, 2007b, 2007c). These characteristics are of importance to control the adsorption of various adsorbates (water, metal ions, low-molecular organics, polymers, proteins, etc.), chemical modification of oxide surface, filling of polymers by nanooxides, aggregation and re-arrangement of particles in aqueous suspensions, thickening characteristics, features of the interfacial behavior of water and other liquids, interaction with cells and tissues, etc. because of wide utilization of nanooxides in industry, medicine and biotechnology (Iler 1979; Legrand 1998; Basic Characteristics of Aerosil 1997; Alyushin and Astakhova 1971; Chuiko 2003). Any mechanical or mechanochemical treatment of nanooxide powders leads to significant rearrangement of ternary and quaternary particles and partial rearrangement of secondary particles resulting in changes in the specific surface area (S_{BET}), the adsorption capacity (V_p), adsorption-desorption of water (Gun'ko et al. 2003). Treatments of wetted powders or suspensions, drying and heating of them can also change the morphology of primary nanoparticles. The S_{BET} and V_p values and the pore size distributions (PSD) calculated as voids between primary spherical nanoparticles depend also on treatment temperature because of changes in particle binding one to another and water desorption from both surface and volume of primary particles (Iler 1979; Legrand 1998; Basic Characteristics of Aerosil 1997; Chuiko 2003). Both Van der Waals and electrostatic interactions can be detected on the interaction of oxide nanoparticles, and long

V.M. Gun'ko (✉)
Institute of Surface Chemistry, 17 General Naumov Street, Kiev 03164, Ukraine
e-mail: gun@voliacable.com

R. Leboda · J. Skubiszewska-Zięba
Faculty of Chemistry, Maria Curie-Skłodowska University, 20031 Lublin, Poland

and short range interactions can be modified by the surface coating with another oxide, organic functionalities, etc. The formation of the chemical bonds between adjacent nanoparticles is possible on dehydration on heating. Heating strongly affects the structural characteristics of porous silicas (Iler 1979; Legrand 1998). For instance, SBA-16 silica exhibits relatively high thermal stability up to 1173 K; however, an increase in the calcination temperature results in a decrease of the BET surface area and volume of pores (Grudzien et al. 2007). Fumed silica has high temperature stability (Basic Characteristics of Aerosil 1997). Features of hydration-dehydration of particles depend on the chemical composition of them and the structural and textural characteristics of the powders; therefore, thermal and hydration/dehydration treatment results for individual and composite fumed oxides can be different on the same treatment conditions. The aim of this paper was to compare structural and adsorptive characteristics of individual and composite nanooxides and to search regularities in the temperature dependences of these characteristics.

2 Materials and methods

The structural characteristics of fumed silicas (A-100, A-150, A-300), alumina (Al_2O_3), and mixed fumed oxides Al_2O_3/SiO_2 (SA5 and SA96, i.e. with low and high content of alumina) and $Al_2O_3/SiO_2/TiO_2$ (AST with high content of alumina and low content of silica and titania) (Table 1) were analyzed here. Another set of fumed oxides (A-50, A-100, A-200, A-300, A-400, A-500, Al_2O_3, TiO_2, SA1, SA3, SA23, SA30, ST9, ST14, ST20, ST29, AST50) (pilot plant at the Institute of Surface Chemistry, Kalush, Ukraine) described in detail previously (Gun'ko et al. 2001, 2003, 2005, 2007a, 2007b, 2007c), silica gels Si-40, Si-60 and Si-100 (Merck) (Gun'ko et al. 2002), mesoporous ordered silicas (MCM-41, MCM-48, SBA-15) (Gun'ko et al. 2007b) were used for comparative characterization. Chemical composition of mixed fumed oxides (Table 1) was analyzed using a XRF (Canberra, USA) spectrophotometer with a ^{55}Fe (or ^{109}Cd) radioactive source and an amplitude analyzer (Canberra) coupled with a computer with the AXIL program. Before the XRF measurements all samples were heated at 723 K for 8 h to remove adsorbed compounds and residual HCl and MCl groups remaining after pyrogenic synthesis in the $O_2/H_2/N_2$ flame using precursors MCl_n (M = Si, Al, Ti). The synthesis of similar individual and composite nanooxides was described previously (Basic Characteristics of Aerosil 1997; Gun'ko et al. 2001, 2005, 2007a, 2007b, 2007c).

To analyze the structural characteristics of fumed oxides, low-temperature (77.4 K) nitrogen adsorption–desorption isotherms were recorded using Micromeritics ASAP 2010 and 2405N adsorption analyzers. The specific surface area (S_{BET}) was calculated according to the standard BET method (Gregg and Sing 1982). The total pore volume V_p was evaluated by converting the volume of nitrogen adsorbed at $p/p_0 = 0.98 - 0.99$ (p and p_0 denote the equilibrium pressure and the saturation pressure of nitrogen at 77.4 K, respectively) to the volume of liquid nitrogen per gram of adsorbent. The nitrogen desorption data were utilized to compute pore size distributions (PSDs) (differential $f_V(R_p) \sim dV_p/dR_p$ and $f_S(R_p) \sim dS/dR_p$) (Nguyen and Do 1999; Gun'ko and Do 2001) using a model of pores as voids between spherical nanoparticles and a regularization procedure (Provencher 1982) under non-negativity condition ($f_V(R_p) \geq 0$ at any R_p) at a fixed regularization parameter $\alpha = 0.01$. For a pictorial presentation of the pore

Table 1 Composition and structural characteristics of fumed oxides pre-heated at different temperatures

Oxide	C_{SiO_2} wt%	$C_{Al_2O_3}$ wt%	C_{TiO_2} wt%	$S_{BET,373\ K}$ m^2/g	$S_{BET,473\ K}$ m^2/g	$S_{BET,623\ K}$ m^2/g	$V_{p,373\ K}$ cm^3/g	$V_{p,473\ K}$ cm^3/g	$V_{p,623\ K}$ cm^3/g
A-300	99.9			318	331	195	0.695	0.689	0.371
A-150	99.9			128	152	206	0.514	0.408	0.294
A-100	99.9			80	92	63	0.158	0.155	0.161
Al_2O_3		99.8		100	107	103	0.224	0.281	0.194
Al_2O_3		99.8		91	95	92	0.197	0.220	0.248
Al_2O_3		99.8		79	89	73	0.134	0.167	0.177
Al_2O_3		99.8		81	86	81	0.206	0.188	0.156
SA5	94.6	5.3	0.1	261	266	234	0.623	0.719	0.637
SA96	3.8	96.1	0.1	80	81	75	0.149	0.163	0.138
AST1	10.0	89.0	1.0	81	99	108	0.199	0.253	0.253
AST06	20.0	79.4	0.6	78	97	96	0.208	0.234	0.153
AST03	2.75	97.0	0.25	80	125	121	0.307	0.308	0.224

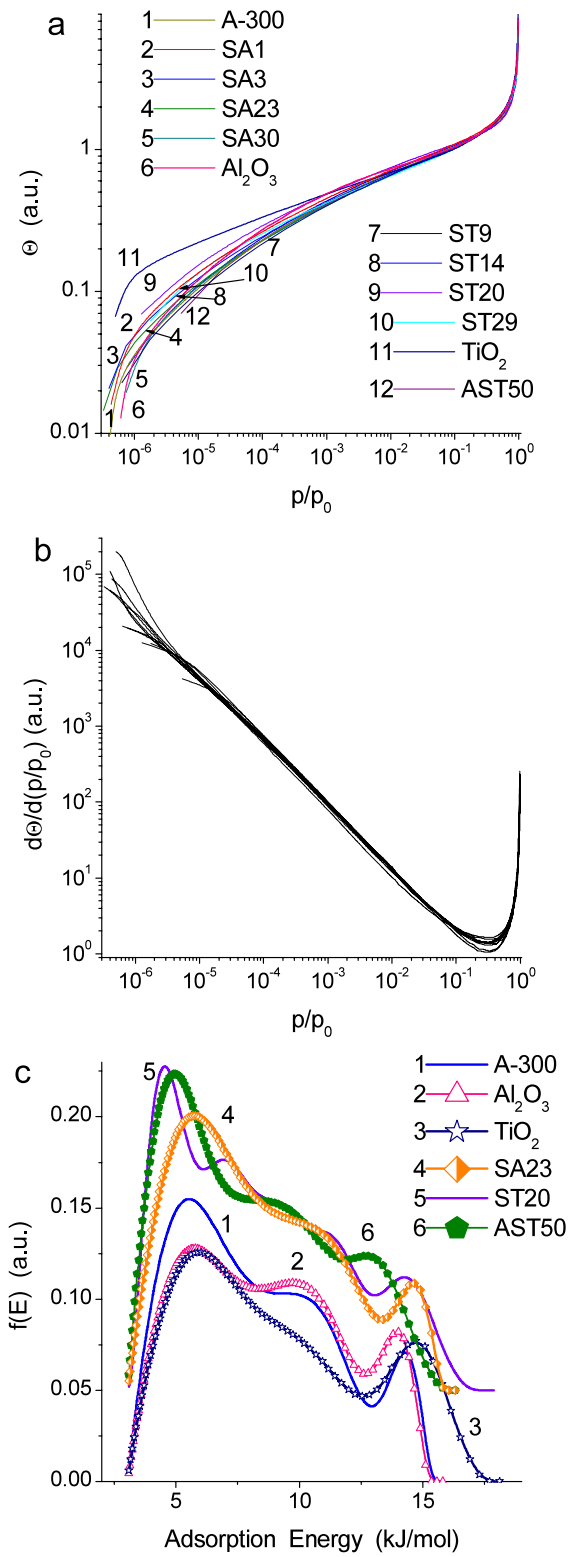

Fig. 1 (**a**) Relative adsorption of nitrogen ($\Theta = a/a_m$) and (**b**) derivatives $d\Theta/d(p/p_0)$ as function of relative pressure; and (**c**) adsorption energy distributions $f(E)$ for set of fumed oxides (A-300, Al_2O_3, TiO_2, SA1, SA3, SA23, SA30, ST9, ST14, ST20, ST29, AST50)

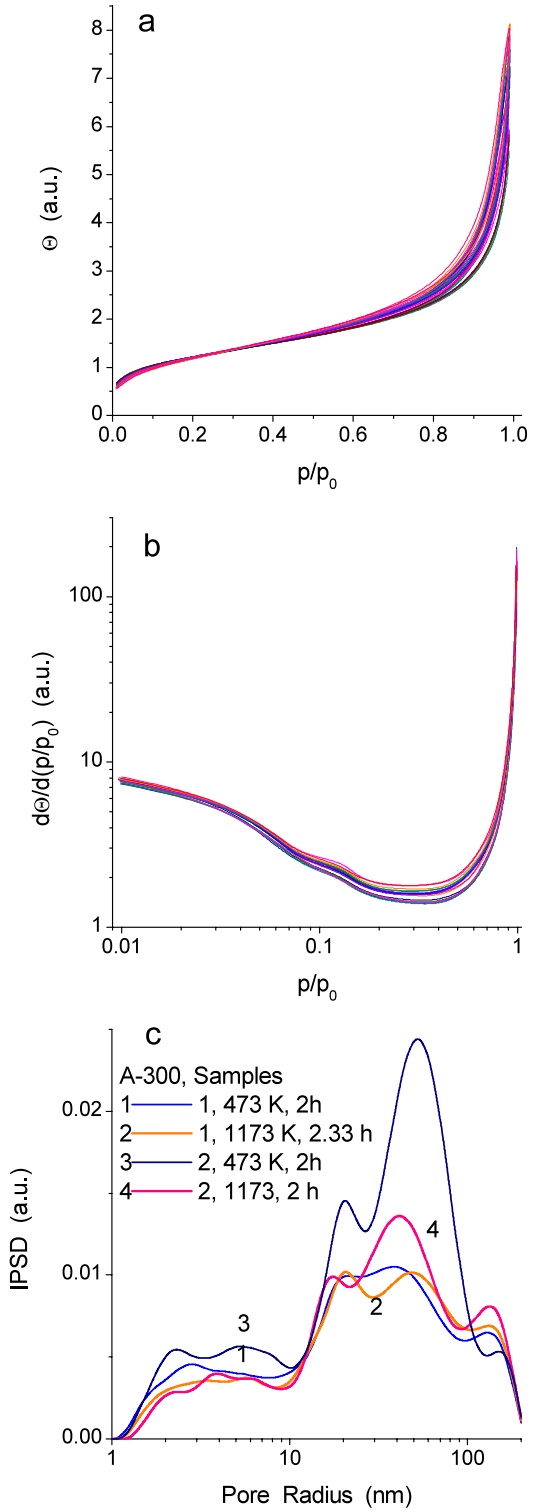

Fig. 2 (**a**) Relative adsorption of nitrogen ($\Theta = a/a_m$) and (**b**) derivatives $d\Theta/d(p/p_0)$ as function of relative pressure; and (**c**) DFT IPSD (model of voids between spherical particles) for two samples of A-300 (weight loss of 3.2 and 1.3 wt% on heating to 1173 K and bulk density of 0.024 and 0.028 g/dm^3, respectively) heated at different temperatures (473, 573, 873, and 1173 K) for different time (from 10 min to 5 h)

size distributions, the differential $f(R)$ functions were recalculated to incremental PSDs (IPSDs). The PSDs were also calculated using overall equation within the framework of Density Functional Theory (DFT) (Do et al. 2001) with the same model of pores (Gun'ko et al. 2007c). Calculations of the specific surface area S_φ (at $N = 2.5$, t and r_m at $0.05 < p/p_0 < 0.2$) were carried out with equation (Gun'ko et al. 2007c)

$$S_\varphi = \int_{a_{\min}}^{a_{\max}} \frac{3}{2a^3\rho}\left[2(a+t)^2 + Nr_m \arcsin\left(\frac{a}{a+t+r_m}\right) \times\sqrt{(a+t+r_m)^2 - a^2} - N(a+t)\left(\frac{ar_m}{a+t+r_m} + t\right)\right]\varphi(a)\mathrm{d}a \quad (1)$$

where a is the particle radius, ρ is the silica density, N is the average coordination number of primary particles in aggregates, t is the thickness of an adsorbed nitrogen layer, r_m is the meniscus radius corresponding to radius of void between spherical particles, and $\varphi(a)$ is particle size distribution (PaSD) calculated using the self-consisting regularization procedure for $f_V(R)$ and $\varphi(a)$ with the model of voids between spherical nanoparticles. An additional rigid criterion $|S_\varphi - S_{BET}| < 0.5$ m^2/g was used to determine the $a_{\min}$ and $a_{\max}$ values for the $\varphi(a)$ distributions calculated at $p/p_0 < 0.5$. The $f_V(R)$ and $f_S(R)$ functions were used to calculate contributions of micropores (S^*_{mic}, V_{mic}) at $R < 1$ nm, mesopores (S^*_{mes}, V_{mes}) at $1 < R < 25$ nm, and macropores (S^*_{mac}, V_{mac}) at $25 < R < 200$ nm to the specific surface area and the total porosity. Additionally, $f_S(R)$ was used to estimate deviation of the pore shape from the model of pores

$$\Delta w = \frac{S_{BET}}{\int_{R_{\min}}^{R_{\max}} f_S(R)\mathrm{d}R} - 1 \quad (2)$$

where $R_{\max}$ and $R_{\min}$ are the maximal and minimal pore radii respectively. The S^*_{mic}, S^*_{mes} and S^*_{mac} values were corrected by multiplication by $(\Delta w + 1)$ that gives $S^*(\Delta w + 1) = S_{sum} = S_{mic} + S_{mes} + S_{mac} = S_{BET}$.

The Fowler-Guggenheim (FG) equation describing localized monolayer adsorption with lateral interaction was used as a local isotherm θ_l in the overall adsorption isotherm to calculate the adsorption energy distribution $f(E)$ (Jaroniec and Madey 1988; Choma and Jaroniec 1997).

3 Results and discussion

The morphology of primary nanoparticles as well as of particles of higher hierarchic levels is typical and nearly the same for all individual and complex fumed oxides. This results in the same shape of normalized adsorption isotherms $\Theta(p/p_0)$ (Fig. 1a) despite the difference in the PaSDs as well as in the S_{BET} values. This similarity is better seen for derivatives $\mathrm{d}\Theta/\mathrm{d}(p/p_0)$ (Fig. 1b). However, there is some difference in the nitrogen adsorption energy distributions for these nanooxides (Fig. 1c) because of the effects of the chemical structure of silica, alumina, titania and related binary and ternary systems possessing different types and amounts of terminal and bridging hydroxyls of different acidity. For instance, the interaction energy is higher on the adsorption of nitrogen molecules on titania than on silica or alumina due to stronger dispersive, electrostatic (−13.3, −9.5, and −5.4 kJ/mol) and charge transfer (−5.2, −2.9, and −1.6 kJ/mol) interactions in complexes –O–H···N≡N with TiO(H)Ti, SiO(H)Al and SiOH groups, respectively, according to the Kitaura-Morokuma analysis of these complexes using the GAMESS program suit (Schmidt et al. 1993; Granovsky 2007) with the 6-31G(d,p) basis set. Both structural and energetic factors cause a small difference in the nitrogen adsorption at very low pressures $p/p_0 < 10^{-4}$ (Fig. 1a). Notice that these factors can more strongly affect the adsorption/desorption of water because of its more specific interaction with oxides (Iler 1979; Legrand 1998).

Heating of nanosilica at different temperatures (over the 473–1173 K range) for different time (10 min to 5 h) weakly affects the morphology of particles (Figs. 2a and 2b). In contrast to the nitrogen adsorption on different oxides when their difference appears at low pressures (Fig. 1) heating of nanosilicas leads to a larger difference in the adsorption at higher pressures. This is due to changes in the characteristics of both primary and secondary particles that are well seen for the PSDs (Fig. 2c) more sensitive to heating than the normalized isotherms because these changes are over the total range of the pore size caused by associative desorption of water from both surface and bulk of primary particles. Therefore, the specific surface area depends on treatment

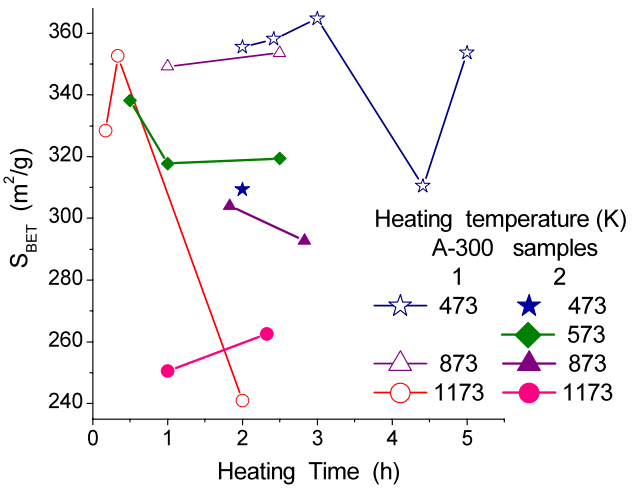

Fig. 3 Changes in the specific surface area of two samples A-300 heated at different temperatures

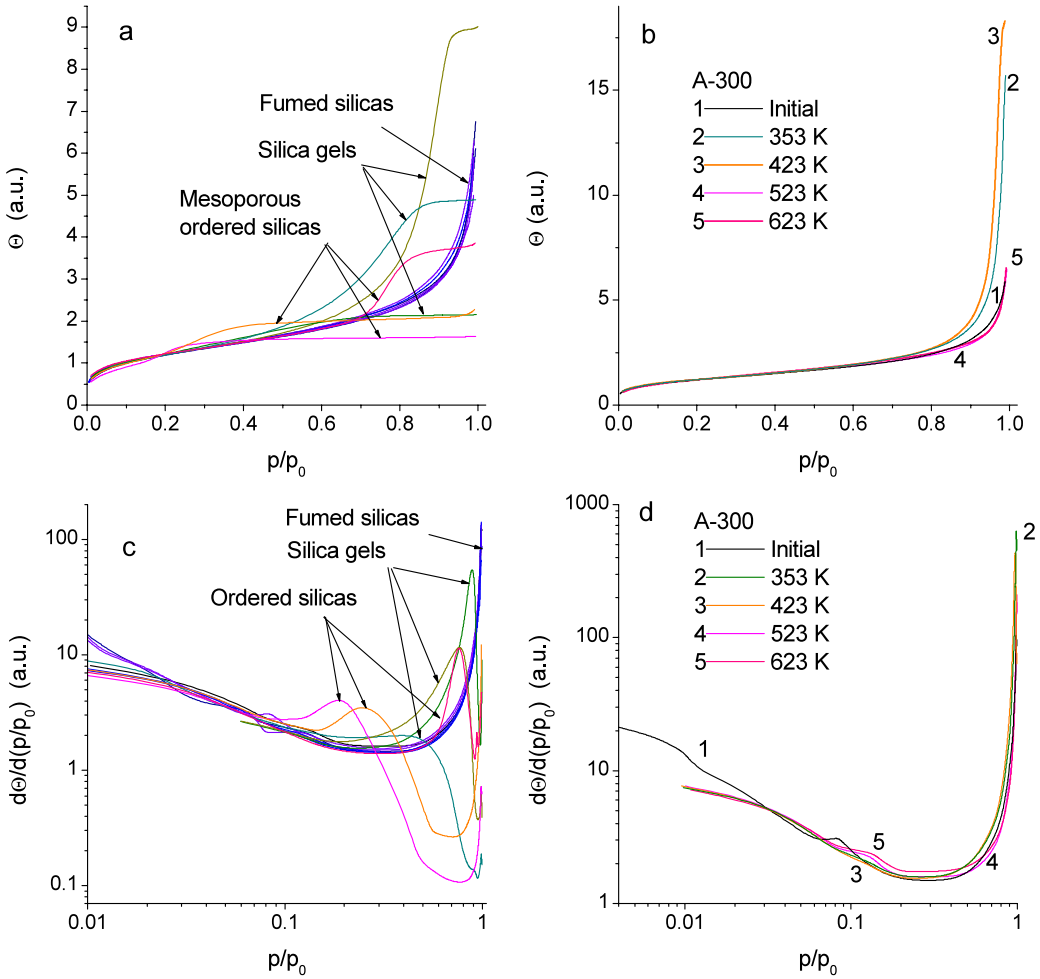

Fig. 4 (**a**, **b**) Relative adsorption of nitrogen ($\Theta = a/a_m$) and (**c**, **d**) derivatives $d\Theta/d(p/p_0)$ as function of relative pressure for (**a**, **c**) fumed silicas (A-50, A-100, A-200, A-300, A-400, and A-500), silica gels (Si-40, Si-60, and Si-100) and mesoporous ordered silicas (MCM-41, MCM-48 and SBA-15); and (**b**, **d**) A-300 initial (1), wetted-dried (2), and dried after hydrothermal treatment at different temperatures (curves 3–5)

conditions (Fig. 3) since the $|\Delta S_{BET}/S_{BET}|$ values change over a wide range up to ~0.3 on heating at 1173 K for 2 h. It should be noted that both $\Theta(p/p_0)$ and $d\Theta/d(p/p_0)$ functions are sensitive to changes in the particle morphology. This is well seen for a set of silicas: fumed silicas—silica gels—mesoporous ordered silicas (Fig. 4). However, these differences appear mainly at $p/p_0 > 0.4$ when capillary condensation starts in mesopores of various shapes, and this effect depends on the PSD and the topology of pores. Additionally, the $d\Theta/d(p/p_0)$ curve shapes differ at $p/p_0 < 0.02$ for porous and fumed silicas (Fig. 4c) due to the presence of narrow pores in the first one in contrast to nanosilicas loosely composed with nonporous primary nanoparticles practically without the formation of micropores ($R < 1$ nm) between them. The presence of pores with a narrow PSD in ordered silicas or silica gels causes appearance of a maximum in the $d\Theta/d(p/p_0)$ curves at $0.2 < p/p_0 < 0.85$ depending on the size of these pores, since the narrower the pores, the lower the pressure of this maximum. Fumed oxides do not have ordered structure of pores; therefore, a similar $d\Theta/d(p/p_0)$ maximum is absent. A similar maximum is absent after hydrothermal treatments of fumed silica A-300 at different temperatures (Fig. 4d) despite significant re-arrangement of primary particles and changes in their size (Gun'ko et al. 2004). Additionally, a similar maximum is absent on suspending of nanosilica ($C_{A-300} = 1$–20 wt%), sonication, drying on air, and heating at 473 K for 2 h. Consequently, fumed oxides are morphologically stable.

Heating of nanooxides at different temperatures and fast subsequent measurements (without relaxation of particles in air) show changes the temperature dependences of the nitrogen adsorption (Fig. 5) and organization of secondary and higher level particles. This results in changes in the relationships between the S and V values (Fig. 6) and the shape of the PSDs (Fig. 7). The textural characteris-

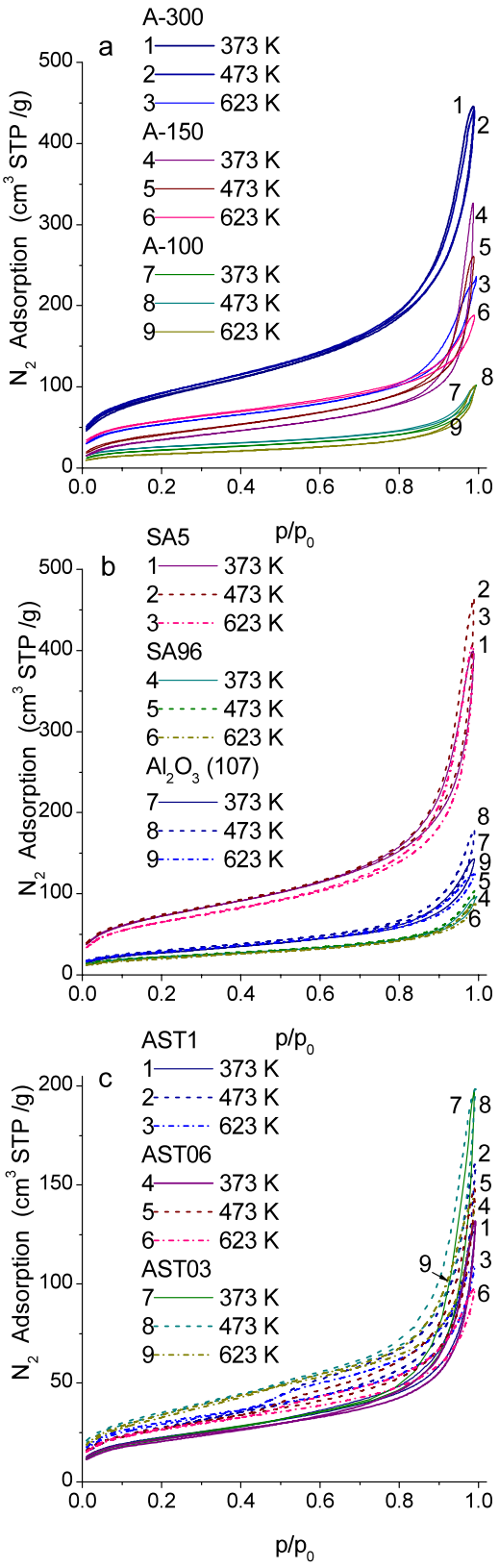

Fig. 5 Nitrogen adsorption-desorption isotherms for (**a**) nanosilicas, (**b**) SA and alumina ($S_{BET,473\ K} = 107\ m^2/g$), and (**c**) AST measured after heating of the samples at different temperatures before the measurements

tics of nanooxide powders depend on the heating temperature, especially macropores, because stronger changes occur in the structure of agglomerates of aggregates than aggregates of primary particles. This reflects in the relationships for macropores (Fig. 6). There is a nearly linear relationship between the specific surface area and the pore volume of meso- and macropores. However, a significant scatter is observed for the relationship between the S_{BET} value and S_{mac} or V_{mac} due to random structures of aggregates and agglomerates and the sensitivity of their organization to heating and any other treatments (Gun'ko et al. 2003, 2004, 2005). As a whole, aggregates of primary nanoparticles are more stable that agglomerates at any mechanical or thermal treatments. Thus, heating of samples at different temperatures more strongly affects the characteristics of macropores (Table 1, Figs. 6 and 7), i.e. voids between secondary particles in ternary particles. Samples with alumina and alumina/silica (SA5 and SA96) are more stable than other nanooxides shown here, and fumed silica possesses a minimal structural and morphological stability. This is due to totally amorphous character of fumed silica in contrast to alumina (γ- and α-phases are observed in the XRD patterns of these samples) and titania (crystalline phase is observed in ST and AST samples, Gun'ko et al. 2005, 2007a). Additionally, associative desorption of water from silica requires stronger changes in the structure of particles than that for alumina or titania because the Si atoms in silica do not have hyperstoichiometric surroundings in contrast to Al and Ti in the Al_2O_3 and TiO_2 phases, respectively.

Several processes occur on heating of nanooxides from room temperature to 1100 K or higher because of molecular and associative desorption of water from the particle surface and volume, and changes in the IPSDs (Fig. 7) and the PaSDs (Fig. 8) reflect these processes depending on the chemical composition of nanooxides. Fumed SA and Al_2O_3 demonstrate more stable PSDs (Fig. 7, at $R < 20$ nm) and PaSDs (Fig. 8) than silica and AST samples. Maximal changes in the PSD and other structural characteristics are observed for A-300 heated at 623 K (Fig. 7a). Notice that heating of nanosilica at $T > 700$ K can lead to relatively stable structural changes (Gun'ko et al. 2001, 2003) due to the formation of the Si–O–Si bonds between adjacent primary particles since these bonds are hydrolytically stable in contrast to asymmetric bonds such as Si–O–Ti or Si–O–Al.

4 Conclusion

The adsorption isotherms of nitrogen can be used to determine not only the S_{BET} and V_p values and the PSD functions but also the primary particle size distributions using pair integral equations related to PSD and PaSD and solved

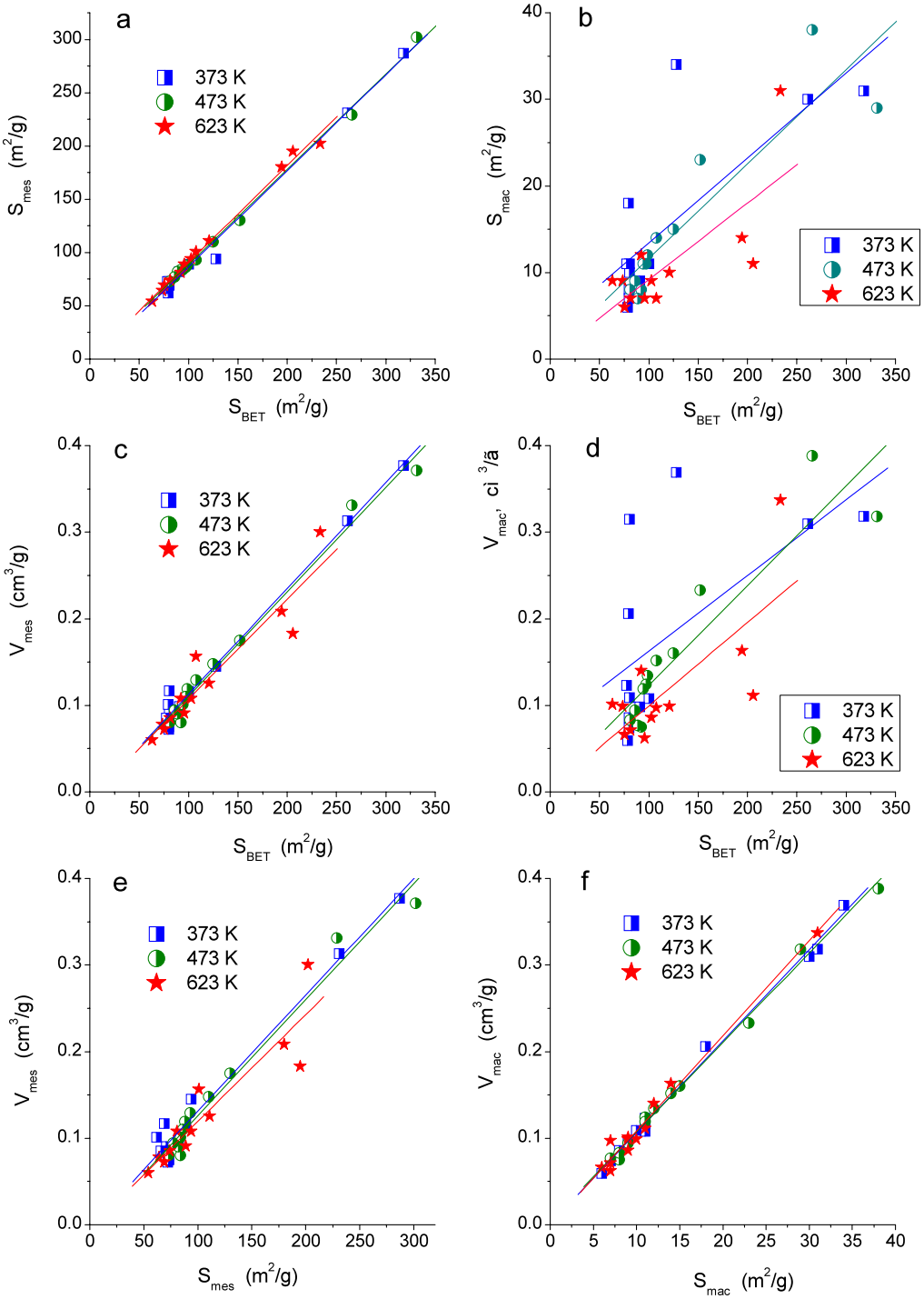

Fig. 6 Relationships between the structural characteristics of fumed oxides heated at different temperatures: S_{BET} and (**a**) S_{mes}; (**b**) S_{mac}; (**c**) V_{mes}; (**d**) V_{mac}; and (**e**) S_{mes} and V_{mes}; (**f**) S_{mac} and V_{mac} (samples shown in Table 1)

with the self-consisting regularization procedure. Heating of nanooxides caused several processes (such as dehydration of the surface and the bulk of primary particles, binding of adjacent nanoparticles due to condensation of hydroxyls, rearrangement of secondary and ternary particles) that result in structural changes of nanooxides depending on the heating temperature. As a whole the morphology of primary nanoparticles of fumed oxides is stable on different treatments in contrast to the structure of secondary particles and especially higher level particles.

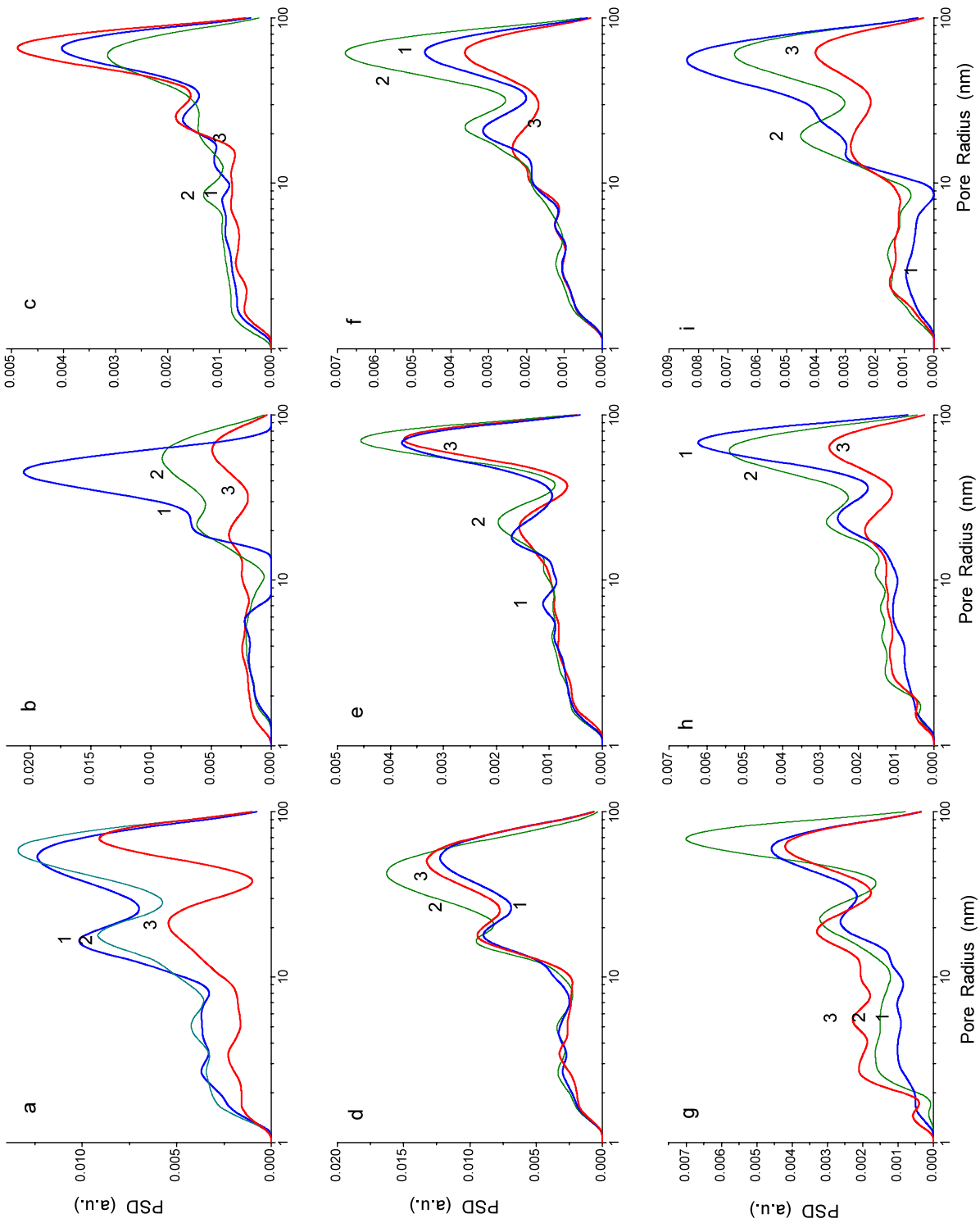

Fig. 7 DFT IPSD$_V$ for fumed oxides heated at different temperatures (curves 1) 373 K, (2) 473 K and (3) 623 K: (**a**) A-300; (**b**) A-150; (**c**) A-100; (**d**) SA5; (**e**) SA96; (**f**) Al_2O_3; (**g**) AST1; (**h**) AST06; and (**i**) AST03

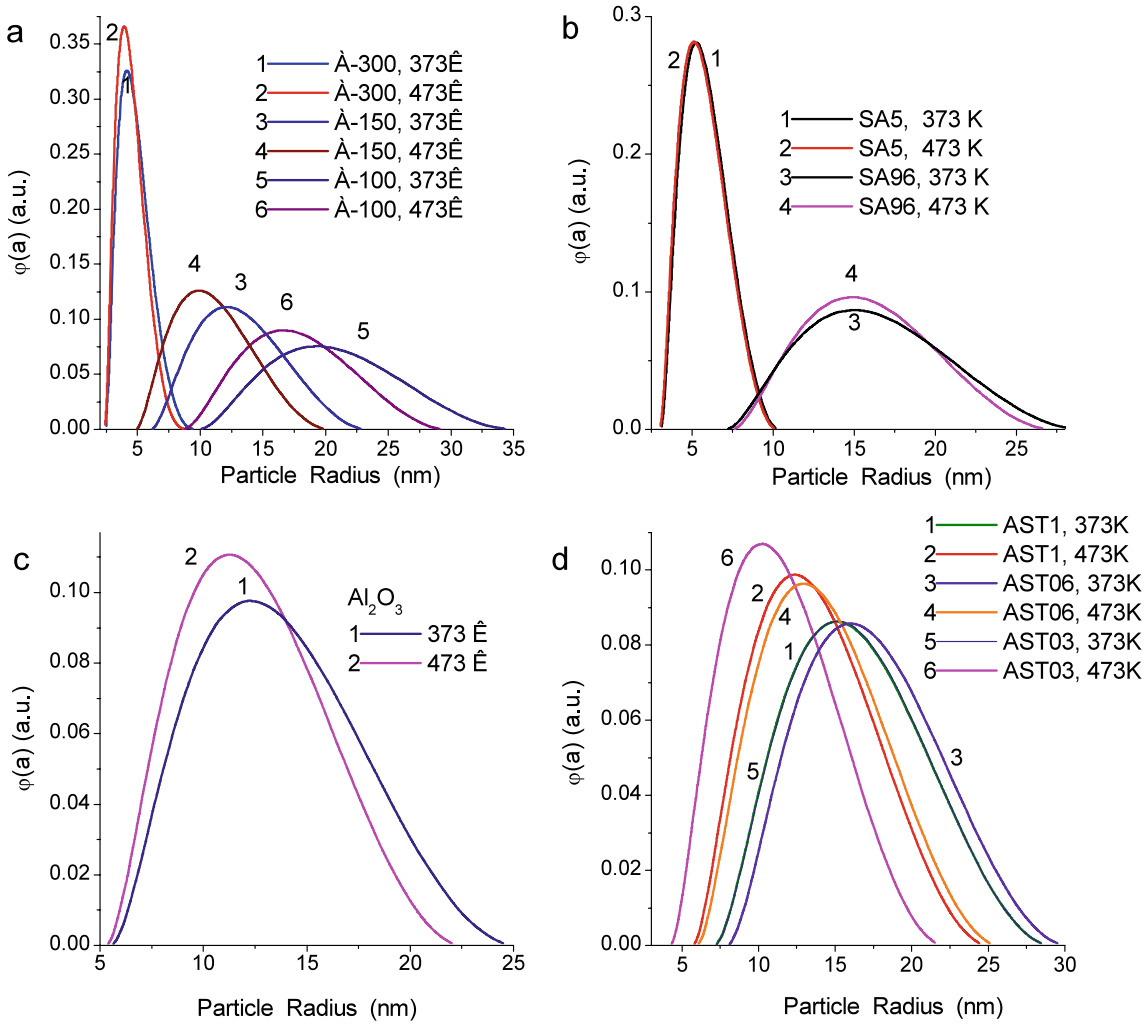

Fig. 8 Primary particle size distributions for fumed oxides heated at different temperatures: (**a**) different silicas; (**b**) SA5 and SA96; (**c**) Al_2O_3; and (**d**) AST

Acknowledgement The authors thank Prof. M. Jaroniec for the nitrogen adsorption measurements for fumed oxides shown in Fig. 1.

References

Alyushin, M.T., Astakhova, M.N.: Aerosil and its application in pharmaceutical practice. Pharmacy **6**, 73–77 (1971)

Basic Characteristics of Aerosil. Technical Bulletin Pigments, No. 11, Degussa AG, Hanau (1997)

Choma, J., Jaroniec, M.: Energetic and structural heterogeneity of synthetic microporous carbons. Langmuir **13**, 1026–1030 (1997)

Chuiko, A.A. (ed.): Medical Chemistry and Clinical Application of Silicon Dioxide. Naukova Dumka, Kiev (2003)

Do, D.D., Nguyen, C., Do, H.D.: Characterization of micro-mesoporous carbon media. Colloids Surf. A **187–188**, 51–71 (2001)

Granovsky, A.A.: PC GAMESS version 7.1. http://classic.chem.msu.su/gran/gamess/index.html (2007)

Gregg, S.J., Sing, K.S.W.: Adsorption, Surface Area and Porosity, 2nd edn. Academic Press, San Diego (1982)

Grudzien, R.M., Grabicka, B.E., Jaroniec, M.: Adsorption studies of thermal stability of SBA-16 mesoporous silicas. Appl. Surf. Sci. **253**, 5660–5665 (2007)

Gun'ko, V.M., Do, D.D.: Characterization of pore structure of carbon adsorbents using regularization procedure. Colloids Surf. A **193**, 71–83 (2001)

Gun'ko, V.M., Mironyuk, I.F., Zarko, V.I., Turov, V.V., Voronin, E.F., Pakhlov, E.M., Goncharuk, E.V., Leboda, R., Skubiszewska-Zięba, J., Janusz, W., Chibowski, S., Levchuk, Yu.N., Klyueva, A.V.: Fumed silicas possessing different morphology and hydrophilicity. J. Colloid Interface Sci. **242**, 90–103 (2001)

Gun'ko, V.M., Dyachenko, A.G., Borysenko, M.V., Skubiszewska-Zięba, J., Leboda, R.: CVD-Titania on mesoporous silica gels. Adsorption **8**, 59–70 (2002)

Gun'ko, V.M., Voronin, E.F., Mironyuk, I.F., Leboda, R., Skubiszewska-Zięba, J., Pakhlov, E.M., Guzenko, N.V., Chuiko, A.A.: The effect of heat, adsorption and mechanochemical treatments on stuck structure and adsorption properties of fumed silicas. Colloids Surf. A **218**, 125–135 (2003)

Gun'ko, V.M., Skubiszewska-Zięba, J., Leboda, R., Khomenko, K.N., Kazakova, O.A., Povazhnyak, M.O., Mironyuk, I.F.: Influence of morphology and composition of fumed oxides on changes in their structural and adsorptive characteristics on hydrothermal treat-

ment at different temperatures. J. Colloid Interface Sci. **269**, 403–424 (2004)

Gun'ko, V.M., Mironyuk, I.F., Zarko, V.I., Voronin, E.F., Turov, V.V., Pakhlov, E.M., Goncharuk, E.V., Nychiporuk, Yu.M., Kulik, T.V., Palyanytsya, B.B., Pakhovchishin, S.V., Vlasova, N.N., Gorbik, P.P., Mishchuk, O.A., Chuiko, A.A., Skubiszewska-Zięba, J., Janusz, W., Turov, A.V., Leboda, R.: Morphology and surface properties of fumed silicas. J. Colloid Interface Sci. **289**, 427–445 (2005)

Gun'ko, V.M., Nychiporuk, Y.M., Zarko, V.I., Goncharuk, E.V., Mishchuk, O.A., Leboda, R., Skubiszewska-Zięba, J., Skwarek, E., Janusz, W., Yurchenko, G.R., Osovskii, V.D., Ptushinskii, Y.G., Turov, V.V., Gorbik, P.P., Blitz, J.P., Gude, K.: Relationships between surface compositions and properties of surfaces of mixed fumed oxides. Appl. Surf. Sci. **253**, 3215–3230 (2007a)

Gun'ko, V.M., Turov, V.V., Turov, A.V., Zarko, V.I., Gerda, V.I., Yanishpolskii, V.V., Berezovska, I.S., Tertykh, V.A.: Behaviour of pure water and water mixture with benzene or chloroform adsorbed onto ordered mesoporous silicas. Cent. Eur. J. Chem. **5**, 420–454 (2007b)

Gun'ko, V.M., Turov, V.V., Leboda, R., Zarko, V.I., Skubiszewska-Zięba, J., Charmas, B.: Adsorption, NMR and thermally stimulated depolarization current methods for comparative analysis of heterogeneous solid and soft materials. Langmuir **23**, 3184–3192 (2007c)

Iler, R.K.: The Chemistry of Silica. Wiley, New York (1979)

Jaroniec, M., Madey, R.: Physical Adsorption on Heterogeneous Solids. Elsevier, Amsterdam (1988)

Legrand, A.P. (ed.), The Surface Properties of Silicas. Wiley, New York (1998)

Nguyen, C., Do, D.D.: A new method for the characterization of porous materials. Langmuir **15**, 3608–3615 (1999)

Provencher, S.W.: A constrained regularization method for inverting data represented by linear algebraic or integral equations. Comput. Phys. Commun. **27**, 213–227 (1982)

Schmidt, M.W., Baldridge, K.K., Boatz, J.A., Elbert, S.T., Gordon, M.S., Jensen, J.J., Koseki, S., Matsunaga, N., Nguyen, K.A., Su, S., Windus, T.L., Dupuis, M., Montgomery, J.A.: J. Comput. Chem. **14**, 1347–1363 (1993)